# On Stability and Dynamics of Milling at Small Radial Immersion

E. Govekar[1] (2), J. Gradišek[1], M. Kalveram[2], T. Insperger[3], K. Weinert[2] (1), G. Stépán[3], I. Grabec[1] (1)
[1]Faculty of Mechanical Engineering, University of Ljubljana, Aškerčeva 6, SI-1000 Ljubljana, Slovenia
[2]Dept. of Machining Technology, University of Dortmund, Baroper Str. 301, D-44227 Dortmund, Germany
[3]Dept. of Applied Mechanics, Budapest University of Technology and Economics, H-1521 Budapest, Hungary

**Abstract**
Stability and dynamics of milling at small radial immersion are investigated. Stability charts are predicted by the Semi Discretization method. Two types of instability are predicted corresponding to quasiperiodic and periodic chatter. The quasiperiodic chatter lobes are open and distributed along the spindle speed axis only, while the periodic chatter lobes are closed curves distributed in the plane of spindle speed and depth of cut. Experiments confirm the stability predictions, revealing the two principal types of chatter, the bounded periodic chatter lobes, and some special chatter cases. The recorded tool deflections in these cutting regimes are studied. The experiments also show that the modal properties of a slender tool may depend on spindle speed.

**Keywords**:
End milling, Stability, Dynamics

## 1 INTRODUCTION

Milling operations with small radial immersion and long slender tools are often required in finish machining of parts with deep pockets and thin walls. Since such flexible tools and parts are very susceptible to chatter vibrations, accurate manufacturing can be assured only by judicious selection of cutting parameters. Prediction of chatter free cutting parameters has been intensively investigated over the last decades [1]. Recently it has been shown that stability properties of milling change significantly at small radial immersions where cutting becomes highly intermittent [2]. Further analytical, numerical and experimental investigations [3][4][5][6] have confirmed that in cases of very small immersion milling the true stability boundary differs significantly from the approximate one predicted by the Single Frequency Solution (SFS) method [7], which is widely used for prediction of chatter-free parameters in milling. The main difference is associated with an additional type of instability which occurs during highly intermittent cutting. This instability is called period doubling or flip bifurcation and causes periodic chatter vibrations. The other type of instability, so far considered as the only one in milling, is called Hopf bifurcation and causes quasiperiodic chatter. Since there is a set of stability lobes associated to the each type of instability, the stability boundary in small immersion milling is composed of two sets of lobes located at different spindle speeds.

This paper reports on results of analytical and experimental investigations of milling stability at small radial immersion. Stability boundaries are predicted by the Semi Discretization (SD) method [8]. They are indeed composed of two sets of stability lobes, respectively corresponding to the quasi-periodic and periodic chatter. However, in contrast to the quasiperiodic chatter lobes that are open and distributed along the spindle speed axis, the periodic chatter lobes are shown to be closed curves distributed in the plane of spindle speed and depth of cut. The stability predictions are confirmed by experiments that reveal the two principal types of chatter and some special chatter cases, and also indicate boundedness of periodic chatter lobes. Tool deflections recorded during the observed motion types are studied in detail. The experiments also show that modal properties of a long and slender tool may depend on spindle speed.

## 2 MATHEMATICAL MODEL OF 2-DOF END MILLING

Consider a 2-dof milling operation sketched in Figure 1.

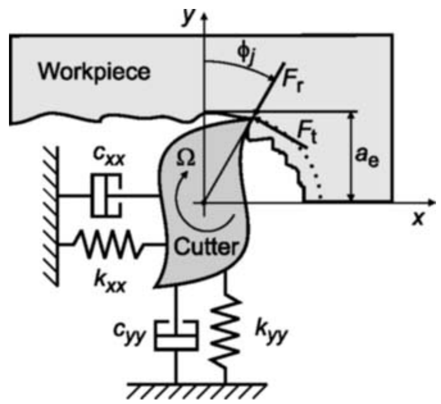


Figure 1: Sketch of 2-dof end milling.

A cutter with $N$ equally spaced teeth rotates at a constant angular velocity Ω. The radial immersion angle of the $j$th tooth varies with time as $\varphi_j(t)=2\pi(\Omega t+(j-1)/N)$. A compliant machine tool structure is excited by the cutting forces at the tool tip causing dynamic response of the structure governed by the following equation:

$$\boldsymbol{M}\ddot{\boldsymbol{X}}(t)+\boldsymbol{C}\dot{\boldsymbol{X}}(t)+\boldsymbol{K}\boldsymbol{X}(t)=\boldsymbol{F}(t) \qquad (1)$$

Here $\boldsymbol{X}$ and $\boldsymbol{F}$ denote the displacement and cutting force vectors, while $\boldsymbol{M}$, $\boldsymbol{C}$, and $\boldsymbol{K}$ denote the mass, damping and stiffness matrices. The cutting force components acting on the $j$th tooth are given by:

$$\begin{aligned} F_{x,j} &= g_j(t)\left(-F_{t,j}(t)\cos\varphi_j(t)-F_{r,j}(t)\sin\varphi_j(t)\right) \\ F_{y,j} &= g_j(t)\left(+F_{t,j}(t)\sin\varphi_j(t)-F_{r,j}(t)\cos\varphi_j(t)\right) \end{aligned} \qquad (2)$$

where $g_j(t)$ is a unit step function determining whether or not the $j$th tooth is cutting. The tangential and radial cutting force components, $F_t$ and $F_r$, are assumed proportional to the chip load defined by the product of chip thickness $h_j(t)$ and depth of cut $a_p$ as:

$$F_{t,j}(t) = K_t a_p h_j(t), \qquad F_{r,j}(t) = k_r F_{t,j}(t) \tag{3}$$

where $K_t$ and $k_r$ respectively denote the specific tangential force coefficient and the force ratio. The chip thickness consists of a static part due to feed, $f_z \sin\varphi_j(t)$, and a dynamic part due to cutter displacement. The stability of cutting is influenced only by the dynamic part of chip thickness given by:

$$h_j(t) = g_j(t)\left(\Delta x \sin\varphi_j(t) + \Delta y \cos\varphi_j(t)\right) \tag{4}$$

where $\Delta x = x(t) - x(t-T)$ and $\Delta y = y(t) - y(t-T)$ describe the surface regeneration, i.e. the difference between the tool positions at the present and previous tooth passes. $T = 2\pi/N\Omega$ denotes the tooth passing period.

Summing the contributions of all cutting edges yields the total cutting force:

$$\begin{bmatrix} F_x(t) \\ F_y(t) \end{bmatrix} = a_p K_t \begin{bmatrix} A_{xx}(t) & A_{xy}(t) \\ A_{yx}(t) & A_{yy}(t) \end{bmatrix} \cdot \begin{bmatrix} \Delta x(t,T) \\ \Delta y(t,T) \end{bmatrix} \tag{5}$$

where $A_{ij}(t)$ denote the time periodic directional dynamic force coefficients (see [7][9] for details). The governing equation of motion of a milling cutter therefore reads:

$$\boldsymbol{M}\ddot{\boldsymbol{X}}(t) + \boldsymbol{C}\dot{\boldsymbol{X}}(t) + \boldsymbol{K}\boldsymbol{X}(t) = a_p K_t \boldsymbol{A}(t)(\boldsymbol{X}(t) - \boldsymbol{X}(t-T)) \tag{6}$$

Time dependence of the directional coefficients $\boldsymbol{A}(t)$ complicates the linear stability analysis of Eq. (6). A possible solution to this problem, followed by the Multi Frequency Solution (MFS) and SFS methods, is to expand $\boldsymbol{A}(t)$ in a Fourier series and retain the terms necessary for the approximation. In the MFS method [6][9], several Fourier terms are retained, whereas in the SFS method [7] only the zeroth order term is kept. The latter approximation is very practical, as it allows a closed form expression of the stability boundary, but it loses accuracy as the radial immersion and the number of cutter teeth decrease, leading to highly intermittent cutting. Alternatively, stability of Eq. (6) can be studied by the recently proposed time domain methods, the Temporal Finite Element Analysis [3][10] or Semi Discretization [3][8] methods. The latter is used in this study and is briefly reviewed below.

## 3 SEMI DISCRETIZATION METHOD

The basic idea of the Semi Discretization method is to discretize the delayed terms of the delay differential equation (DDE) while leaving the current time terms unchanged. This way, the DDE is approximated by a series of ordinary differential equations (ODEs) for which the solutions are known and can be given in closed form [8].

The governing equation of milling (Eq. (6)) is a delayed differential equation with the tooth passing period $T$ as delay. Using $\boldsymbol{Q}(t) = -a_p K_t \boldsymbol{A}(t)$ to simplify the notation, Eq. (6) may be rewritten as:

$$\boldsymbol{M}\ddot{\boldsymbol{X}}(t) + \boldsymbol{C}\dot{\boldsymbol{X}}(t) + (\boldsymbol{K} + \boldsymbol{Q}(t))\boldsymbol{X}(t) = \boldsymbol{Q}(t)\boldsymbol{X}(t-T) \tag{7}$$

Discretization is introduced using a time interval $[t_i, t_{i+1})$ with $t_{i+1} - t_i = \Delta t$. The delay time becomes $T = (m+0.5)\Delta t$, where $m$ is an integer determining the coarseness of the discretization. The periodic coefficient $\boldsymbol{Q}(t) = \boldsymbol{Q}(t+T)$ and the delayed state $\boldsymbol{X}(t-T)$ are approximated by:

$$\begin{aligned} &\boldsymbol{Q}(t) \approx \boldsymbol{Q}_i, \\ &\boldsymbol{X}(t-T) \approx 0.5\left(\boldsymbol{X}_{i-m+1} + \boldsymbol{X}_{i-m}\right) \end{aligned} \tag{8}$$

The DDE in Eq. (7) is herewith transformed into a series of autonomous second order ODEs with $t_i \le t < t_{i+1}$:

$$\boldsymbol{M}\ddot{\boldsymbol{X}}(t) + \boldsymbol{C}\dot{\boldsymbol{X}}(t) + (\boldsymbol{K} + \boldsymbol{Q}_i)\boldsymbol{X}(t) = \frac{\boldsymbol{Q}_i}{2}\left(\boldsymbol{X}_{i-m+1} + \boldsymbol{X}_{i-m}\right) \tag{9}$$

which can be rewritten as systems of first order ODEs:

$$\dot{\boldsymbol{u}}(t) = \boldsymbol{W}_i \boldsymbol{u}(t) + \boldsymbol{V}_i\left(\boldsymbol{u}_{i-m+1} + \boldsymbol{u}_{i-m}\right) = \boldsymbol{W}_i \boldsymbol{u}(t) + \boldsymbol{w}_i \tag{10}$$

with $\boldsymbol{u} = [\dot{x}, \dot{y}, x, y]$. Given the initial condition $\boldsymbol{u}(t_i) = \boldsymbol{u}_i$, the solution of Eq. (10) is:

$$\boldsymbol{u}(t) = e^{\boldsymbol{W}_i(t-t_i)}\left(\boldsymbol{u}_i + \boldsymbol{W}_i^{-1}\boldsymbol{w}_i\right) + \boldsymbol{W}_i^{-1}\boldsymbol{w}_i \tag{11}$$

Substituting $t = t_{i+1}$ and $\boldsymbol{u}(t_{i+1}) = \boldsymbol{u}_{i+1}$ into this solution yields:

$$\begin{aligned} \boldsymbol{u}_{i+1} &= e^{\boldsymbol{W}_i \Delta t}\boldsymbol{u}_i + \left(e^{\boldsymbol{W}_i \Delta t} - \boldsymbol{I}\right)\boldsymbol{W}_i^{-1}\boldsymbol{V}_i\left(\boldsymbol{u}_{i-m+1} + \boldsymbol{u}_{i-m}\right) \\ &= \boldsymbol{P}_i \boldsymbol{u}_i + \boldsymbol{R}_i\left(\boldsymbol{u}_{i-m+1} + \boldsymbol{u}_{i-m}\right) \end{aligned} \tag{12}$$

Eq. (12) can be rewritten as a map: $\boldsymbol{v}_{i+1} = \boldsymbol{Z}_i \boldsymbol{v}_i$, with the state vector $\boldsymbol{v}_i = [\boldsymbol{u}_i, \boldsymbol{u}_{i-1}, \ldots, \boldsymbol{u}_{i-m}]$ and the coefficient matrix:

$$\boldsymbol{Z}_i = \begin{bmatrix} \boldsymbol{P}_i & \boldsymbol{0} & \boldsymbol{0} & \ldots\boldsymbol{0} & \boldsymbol{R}_i & \boldsymbol{R}_i \\ \boldsymbol{I} & \boldsymbol{0} & \boldsymbol{0} & \ldots\boldsymbol{0} & \boldsymbol{0} & \boldsymbol{0} \\ \boldsymbol{0} & \boldsymbol{I} & \boldsymbol{0} & \ldots\boldsymbol{0} & \boldsymbol{0} & \boldsymbol{0} \\ \vdots & \vdots & \vdots & \ddots\vdots & \vdots & \vdots \\ \boldsymbol{0} & \boldsymbol{0} & \boldsymbol{0} & \ldots\boldsymbol{I} & \boldsymbol{0} & \boldsymbol{0} \\ \boldsymbol{0} & \boldsymbol{0} & \boldsymbol{0} & \ldots\boldsymbol{0} & \boldsymbol{I} & \boldsymbol{0} \end{bmatrix} \tag{13}$$

The transition matrix over the principal period $T$ is approximated by coupling the solutions of $m$ successive intervals as:

$$\boldsymbol{\Phi} = \boldsymbol{Z}_{m-1}\boldsymbol{Z}_{m-2}\cdots\boldsymbol{Z}_1\boldsymbol{Z}_0 \tag{14}$$

Finally, stability of the investigated system is determined by the eigenvalues of the transition matrix $\boldsymbol{\Phi}$. The system is stable if all eigenvalues of $\boldsymbol{\Phi}$ are in modulus less than 1. Further details on the semi discretization procedure can be found in [8].

In the case of milling, two possible instabilities can be observed:

1. The critical eigenvalue of $\boldsymbol{\Phi}$ is complex and its modulus is greater than 1. This case corresponds to the Hopf bifurcation causing the quasiperiodic chatter.
2. The critical eigenvalue of $\boldsymbol{\Phi}$ is real and its value is smaller than –1. This case corresponds to the period doubling or flip bifurcation which causes the periodic chatter.

These two instabilities are illustrated in Figure 2 by the eigenvalue trajectories in the complex plane accompanied by the stability chart with the corresponding depth of cut and spindle speed values. In the case of Hopf bifurcation, a pair of complex conjugate eigenvalues penetrates the unit circle in the complex plane, whereas in the case of flip bifurcation, the unit circle is penetrated by one real and negative eigenvalue. More information on bifurcations in dynamical systems can be found in [11].

## 4 RESULTS

The cutting tests were conducted on a high speed milling center using a cylindrical end mill with a single cutting edge ($N$=1), $D$=8 mm diameter, 45 degree helix angle, and $L$=96 mm overhang (L/D=12). A relatively large overhang was used to assure a single dominant vibration mode of the tool, whereas a single edged cutter was used to avoid the disturbances due to tool runout. The purpose of these two